THz-ToF techniques for the detection of inherent discontinuities in dielectric materials based on a SAFT – and an Optical Layer reconstruction algorithm

Holger SPRANGER [1], Jörg BECKMANN [1], Rainer BOEHM [1]
[1] BAM Bundesanstalt für Materialforschung und -prüfung, Berlin, Germany

Contact e-mail: holger.spranger@bam.de

Abstract. Electromagnetic waves with frequencies between 0.1 and 10 THz are described as THz-radiation (T-ray). The ability to penetrate dielectric materials makes T-rays attractive to reveal discontinuities in polymer and ceramic materials. THz-Time Domain Spectroscopy Systems (THz-TDS) are available on the market today which operates with THz-pulses transmitted and received by optically pumped semiconductor antennas. In THz-TDS the travelling time (ToF) and shape of the pulse is changed if it interacts with the dielectric material and its inherent discontinuities. A tomogram of the object under the test can be reconstructed from time of flight diffraction (ToFD) scans if a synthetic focusing aperture (SAFT) algorithm is applied. Otherwise, planar discontinuities like cracks in plastics or delaminated layers in composites can be abstracted as layers located at any angle in relation to the outer sample surface direction. A tomogram from the scanned sample can then be reconstructed in case the interactions of electromagnetic pulses with the existing inherent interfaces are detectable and a model is assumed which describes the device under the test as multilayer structure composed of thin layers with different dielectric properties.
A short description of both the SAFT – and Optical Layer algorithm for the reconstruction of the inherent structure is initially given. Measurements on representative samples with a variety of artificially produced small and large scale. Reconstructed tomograms are presented to discuss and evaluate the benefits and limits of the two different reconstruction approaches.

Introduction

The simultaneous visibility of different dielectrics, drilled holes, air pockets, slits or metallic inlays in structural components can be a challenge for already established volumetric NDT methods. This is especially the case if the composites of the structural component shall be distinguished and quantify with only one test method without any data fusion process. For example X-ray-techniques base on absorption phenomena. Tomographic reconstruction occasionally suffers from too small or too large absorption differences. Plastics and ceramics are sometimes difficult to distinguish radiographically although dual energy procedures have been applied. Common ultrasonic testing methods need a coupling medium to promote the transfer of sound energy into the test specimen. Difficulties arise if a surface structure and experimental and environmental restrictions exist. The strong reflec-

License: http://creativecommons.org/licenses/by-nd/3.0/

tion of the ultrasound signal on interfaces of air filled structures and high absorption effects of plastics can result to a limited penetration of the inspected sample. In contradiction to that electromagnetic waves in the frequency range between 0.1 THz and 10 THz are considered to be a more promising alternative to these techniques. Air as "coupling" medium can be used, dielectric materials and ceramics can be penetrated and distinguished according to the existing complex dielectric or optical refraction properties [1].

The following paper demonstrates and proposes two different approaches for the reconstruction of the inherent structures in polymer parts. It is divided in three sections. First, reconstruction techniques are described briefly. Second, measured and reconstructed data are presented. A short summary and outlook is given at the end.

Reconstruction

Several reconstruction techniques have been already discussed and demonstrated in the context of THz-ToF [2]. Nevertheless, tomographic reconstruction procedures, developed for x-ray computed tomography (CT) applications, have been preferably applied. As a result, reliable tomograms could be presented in case of existing minor refraction property differences between the defect and its surrounding material. Additional geometric artefacts could be observed. The results indicate a strong restriction of the CT application for the inspection of dielectric plastics that engaged us to develop two different reconstruction procedures as described shortly in the following.

Time Domain Synthetic Aperture Focusing Technique (TD-SAFT)

Synthetic Aperture Focusing Technique (SAFT) is a run time based reconstruction method [3]. Basically, a mathematically formulated back projection algorithm is applied to create the SAFT image by using the run time data [4]. The algorithm bases on the analysis of the propagation of electromagnetic waves in dielectric media and the description of structural inhomogeneities or defects in the region of interest (ROI) by means of small point sources. The last approach results from the mathematical assumption that only diffuse scattering will occur when the probe pulse excites the point scatterer. The principle of the SAFT technique and the image reconstruction is presented in Figure 1. The sample under test is scanned along the x-axis (Figure 1 left). A scattered signal is measured (Figure 1 middle) for a locally defined source receiver combination. The position of the scatterer is reconstructed in the SAFT image (Figure 1 right).

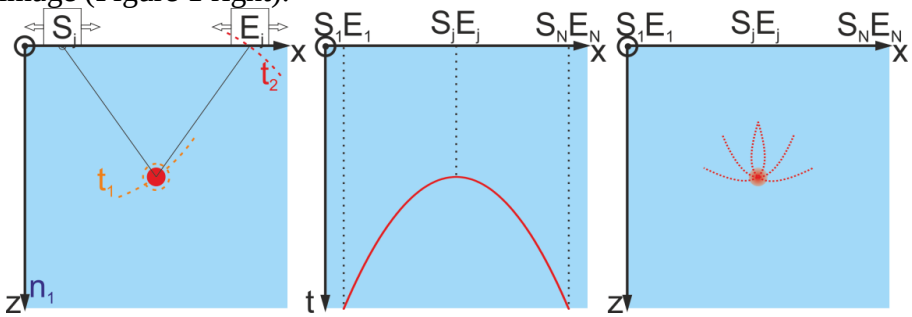

Figure 1 Scheme of measurement and SAFT image reconstruction

left: Source S_j at the position $R_{s,i}$ sends a signal, which hits a point source at time t_1. The scattered signal is measured by the receiver E_i at its position $R_{R,i}$ at the time t_2

middle: B-Scan for different S/R positions $\{R_{s,i}, R_{R,i}\}$, i= 1, 2,..j,..N, with constant relative distances (R_{si},-R_{Ri})

right: local position of the point source computed via SAFT (superposition of hypothetic runtime parabolas)

For the reconstruction procedure the ROI is divided into pixel (2D) or voxel (3D) respectively. A hypothetic scatterer in each pixel is assumed. The next and most important step of SAFT is the calculation of runtimes T to each pixel P_{jk} for each S/R position $(\vec{R}_S, \vec{R}_R)$ taking a refractive index distribution N into account. It seems to be simple for a homogenous and isotropic medium but can be difficult for instance in case of changing refractive indices due to different interfaces, as demonstrated in Figure 2.

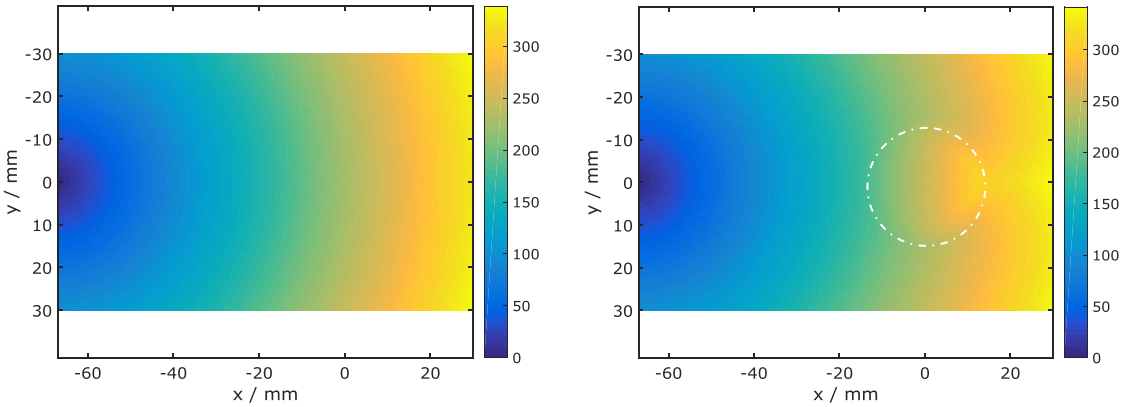

Figure 2: Runtime map for different refractive index profiles for a point source located at R_s (-65, 0)
left: Point-source in air;
right: point source in front of a PE (n=1.5) cylinder (r=15 mm) located at M=(0,0) (white circle)

With T it is possible to assign for every pixel and for every relevant S/R position the measured data sets. The assigned data sets are summed according to equation (1). Signals from different S/R positions were superposed constructive or destructive by this way. Constructive interference takes place at the position P_{jk} if a real scatterer exists in the pixel (voxel), destructive, if not. Hence a SAFT image is reconstructed that indicates the scatterrer at the correct position (see example Figure 1 right).

$$E\left(P_{jk}\right) = \sum_{m=1}^{M}\sum_{n=1}^{N} E_{measured}\left(\vec{R}_{S,m}, \vec{R}_{R,n}, t = T\left(\vec{R}_{S,m}, \vec{R}_{R,n}, N, P_{jk}\right)\right) \tag{1}$$

The described algorithm was adapted to THz-TDS measurements and fully implemented in matlab. It operates in five steps

i. Post processing: Offset correction etc.
ii. Definition of the region of interest: Location of source and receiver, description of known interfaces (surface of the sample)
iii. Calculation of the run time map depending on source and receiver location, map of refractive index, symmetries
iv. Assignment of measured data to reconstruction volume
v. Post processing: envelope calculation etc.

The developed algorithm can be applied on two dimensional as well as three dimensional reconstructions. The measured THz TDS signal is proportional to the real part of the electromagnetic field and requires no further signal processing to fulfil the SAFT requirements for image reconstructions with high signal to noise ratios (SNR). Nevertheless, due to usage of divergent sources, the SNR of measured signals are smaller than for focused setups.

Time Domain Optical Layer Reconstruction (TD-OLR)

Above mentioned SAFT algorithm assumes a distribution of small scatterers located inside the tested sample and doesn't include multiple reflexions. Another approach to reconstruct

data sets could be the description of dielectric samples by means of multilayer structures [5]. The principles of optics could be exploited for the image reconstruction. Large scale defects like delamination could be described as an additional layer located with a given angle in relation to the sample surface inside the test specimen. Based on the optics of multilayer systems, a reconstruction algorithm could be derived, which uses the refractive index, the layer thickness, the polarization state and the incident angle.

The reflection response Γ_1 of a multilayer structure can be described according to [6] in terms of the penetrating field E_1^+ and the reflected field E_1^- as described in equation (2)

$$\Gamma_1 = \frac{E_1^-}{E_1^+} \tag{2}$$

In case of a dielectric slab (Figure 3) Γ_1 can be expressed as

$$\Gamma_1(k) = \frac{\rho_1 + \rho_2 e^{-2ik_1 l_1}}{1 + \rho_1 \rho_2 e^{-2ik_1 l_1}} \tag{3}$$

with Fresnel coefficients $\rho_{1,2}$ and $\tau_{1,2}$ of the front- and backside respectively, the layer thickness l_1 and the corresponding wave length $k_1 = 2\pi\lambda_1^{-1}$

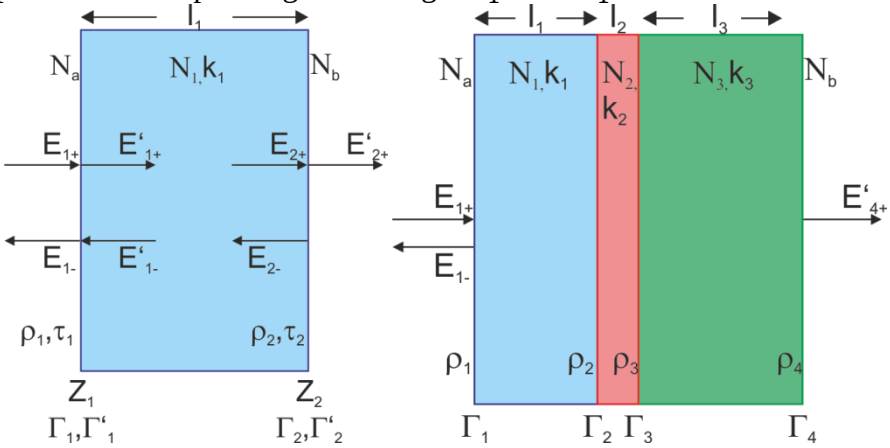

Figure 3: Sketch of transmitted and reflected electromagnetic field components across interfaces of two different dielectric multilayer models

left: slab with characteristic electromagnetic field quantities and material properties

right: structure out of a three layer model, for example a two layer composite with an air layer located in between

Equation (3) is the summation of the geometric series and can be expressed as follows in equation (5)

$$\Gamma_1(\omega) = \rho_1 + \sum_{n=1}^{\infty} (1-\rho_1)^2 (-\rho_1)^{n-1} \rho_2^n e^{-i\omega n T_1} \tag{4}$$

Equation (4) also describes the frequency dependent pulse response as function of $T_{i=1}$ by setting

$$2k_i l_i = \omega T_i \quad \& \quad T_i = \frac{2 l_i N_i}{c_0} \tag{5}$$

Where T_1 is runtime of the wave front back and force through the slab, c_0 is the speed of light and N_1 is the refractive index of the slab material (Figure 3 left).

To calculate the time domain signal response of a slab equation (4) must be transformed via inverse Fourier transformation. As shown in equation (6), the time domain impulse response is expressed by a sum of delta functions, in case absorption is negligible and the real part of N is constant in the frequency range.

$$\Gamma_1(t) = \rho_1\delta(t) + \sum_{n=1}^{\infty}(1-\rho_1)^2(-\rho_1)^{n-1}\rho_2^n\delta(t-nT_1) \tag{6}$$

The reflected field E_1^- is the result of the convolution of the incident field E_1^+ with Γ_1 (equation (6))

$$E_1^-(t) = \rho_1 E_1^+(t) + \sum_{n=1}^{\infty}(1-\rho_1)^2(-\rho_1)^{n-1}\rho_2^n E_1^+(t-nT_1) \tag{7}$$

The equation (7) describes the sum over all multi reflection processes in a dielectric slab. Hence it is possible to allocate the measured reflected pulses to their reflection process in respect to the ToF.

The presented approach can be extended to a multilayer structure as described in (Figure 3). The reflection response of the j-th slab can be expressed in analogy to equation (3)

$$\Gamma_j(k) = \frac{\rho_j + \Gamma_{j+1}e^{-2ik_j l_j}}{1+\rho_j\Gamma_{j+1}e^{-2ik_j l_j}}, \qquad j = M, M-1, \ldots 1 \tag{8}$$

$$\Gamma_{M+1} = \rho_{M+1}$$

M is the number of layers. It equals to 3 in the corresponding selected model in Figure 3. Similar to the above described procedures equation (8) is equal to equation (9)

$$\Gamma_j(\omega) = \rho_j + \sum_{n=0}^{\infty}(1-\rho_j^2)(-\rho_j)^{n-1}\Gamma_{j+1}^n e^{-i\omega T_j} \tag{9}$$

A criterion must be defined to reduce the summations in (9) for multilayer models.
One could be the definition of the number of reflection and transmission processes which take place during the travel of an incident pulse through the whole multilayer structure.
Another one could be the number of transmissions and reflections which results in amplitude drop of the incident pulse below a certain value. A third criterion could be expected runtimes and experimentally limited time windows. In that case only certain runtime combinations will be taken into account. The first and second criteria were preferred for the evaluation of our experiments on multilayer systems. In case of a three layer model (Figure 3) it takes six transmissions and one reflection for the pulse to travel from one side through the layers back to the front. If a Fresnel coefficient of 0.5 for each boundary is assumed, the outgoing pulse amplitude drops up to 0.8% of its initial value. If the sum is limited in equation (9) for that case, it is possible to allocate each detected pulse to a specific runtime (ToF) and amplitude according to equation (10).

$$\begin{aligned}\Gamma_1 = {} & \delta(t)\rho_1 \\ & + (1-\rho_1^2)\left[\delta(t-T_1)\rho_2 + (1-\rho_2^2)\left\{\delta(t-(T_1+T_2))\rho_3 + (1-\rho_3^2)\rho_4\delta(t-(T_1+T_2+T_3))\right\}\right] \\ & + (1-\rho_1^2)\left[\rho_2\rho_3^2\delta(t-(T_1+2T_2)) + \rho_1\rho_2^2\delta(t-2T_1)\right] \\ & + (1-\rho_1^2)\left[2(1-\rho_2^2)\rho_1\rho_2\rho_3\delta(t-(2T_1+T_2)) + \rho_1^2\rho_2^3\delta(t-3T_1)\right] \\ & + O(\rho^8)\end{aligned} \tag{10}$$

The thickness of the second layer (delamination) could be determined from the ToF differences in case the refractive index of it is known. It is also possible to adopt the above procedure for different incident angles and polarization states (pol). As shown in Figure 4, the ToF is changed with the incident angle. The amplitudes of the pulses are influenced by the Fresnel coefficients, which are a function of refraction index and angle of incident. Each interface between the different layers initiates the formation of a pulse. The benefit of the reconstruction approach is the optical description of a layered structure with an analytical

derived recursion formula. This recursion was implemented in matlab first to simulate data for an existing layer model, to compare them with measured data and finally to reconstruct the unknown structures by means of the assumed layer situation.

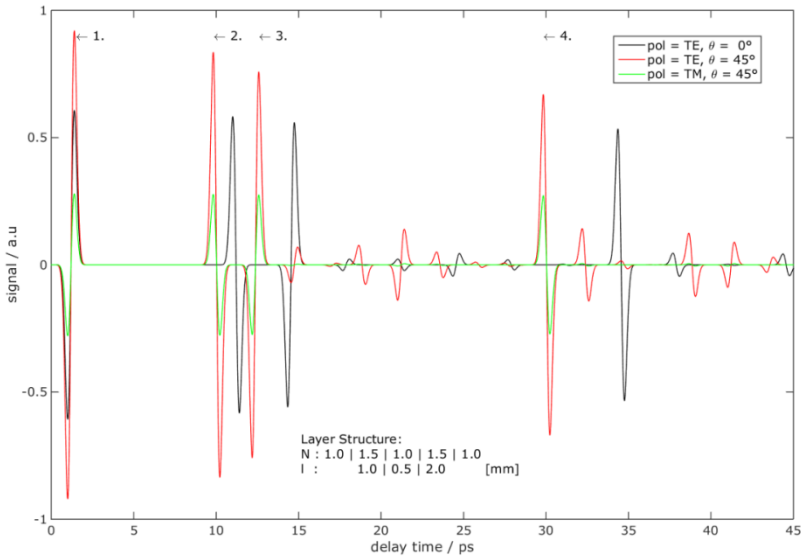

Figure 4: Pulse propagation through a three layer structure

Model for two different angles of incident and polarization states calculated with equation (8) and subsequently transformed via inverse Fourier transformation into the time scale. Numbers 1 to 4 describe the by means of equation (10) allocated pulses initiated at different interfaces between the layers

Experiments and Results

Experimental Setup

Two different types of samples were tested: Cuboids with several slits and a cylinder with drilled holes. The drilled holes were empty or filled with copper wires (Figure 5). All test samples were prepared from the similar high density Polyethylene (PE) block.

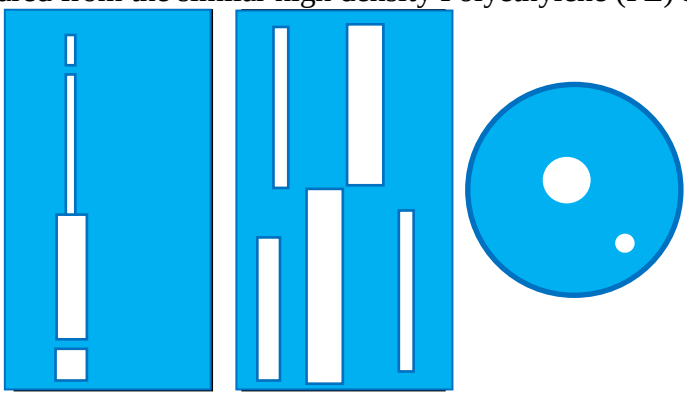

Figure 5: Sketch of the samples under test

Cuboids are 80mm x 40 mm and cylinder is r=15 mm.

All samples are made of PE, it is possible to fill the drilled holes and slits with metals, liquids etc.

All measurements were done with a commercially available Picometrix T-Ray 2000 THz-Time Domain Spectrometer. THz-pulses are generated and detected with two antennas made of GaAs fed by an 800 nm femto-second pulsed laser. A Si beam splitter was used to treat the source and receiver as one unit (BSU). This has few disadvantages. There exists a

power loss of factor four. Multiple reflections in the beam splitter result in a couple of pulses. A pulse train is detected, instead of one pulse only after the reflection at a mirror (Figure 6).

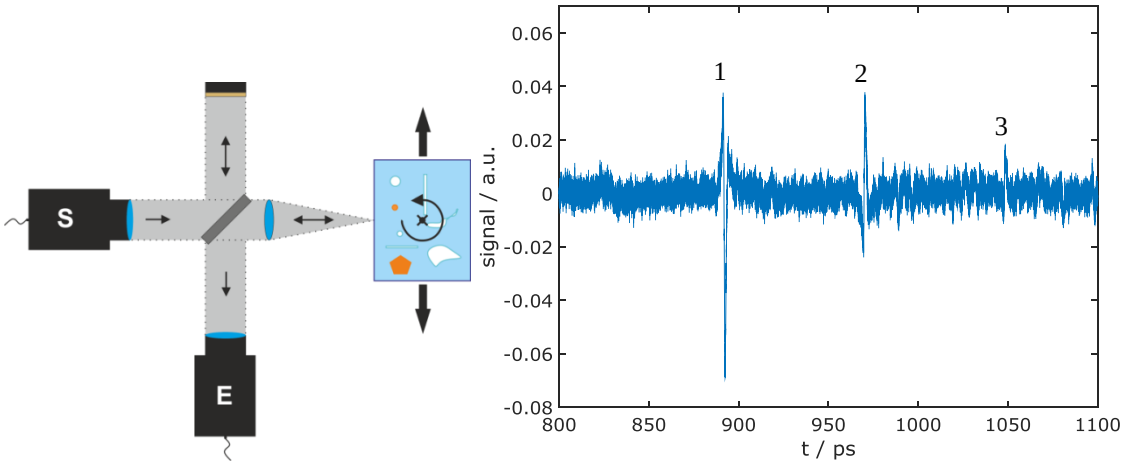

Figure 6: Experimental setup and detected signal after reflection at a gold mirror
left: source and receiver can be treated as one unit, when one uses a beam splitter (gray box) the gold mirror is only used for calibration, lens was used for focusing (focused BSU)
right: pulse train due to the use of a beam splitter unit (BSU) – three pulses appear at reflection at one interface

A manipulation unit has been installed to rotate the sample around a fixed rotation axis and to move it perpendicular to the beam direction. So it was possible to measure the sample on previously defined raster positions. A focussing lens was added behind the beam splitter unit to collimate the beam in a small spot with known phase front. The focal spot was treated as virtual source and receiver position for the reconstructions.

SAFT Reconstruction

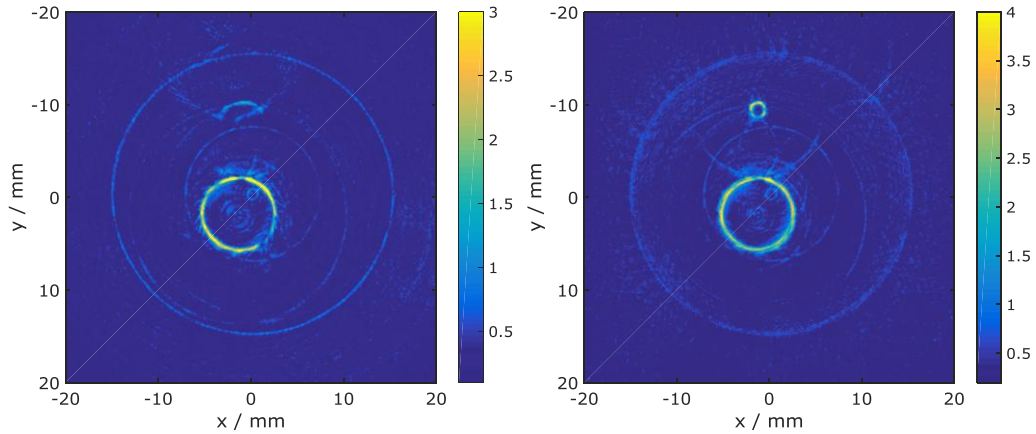

Figure 7: The influence of the refractive index profile on the SAFT reconstruction of a cylindrical sample with embedded copper wires
left: total reconstruction area was assumed to have only one constant index (n=1.5)
right: reconstruction area consists of cylindrical PE matrix (n=1.5) and air (index profile)

Figure 7 shows the SAFT images of the cylindrically shaped sample consisting of a PE matrix and two embedded copper wires with different diameter (Figure 5 right). As discussed above an appropriated time map must be used for the SAFT reconstruction. The time map can take in a first approach a homogenous reconstruction area into account. In that case only the large wire is visible in the reconstruction as shown in Figure 7 (left). Unfortunately, its dimensions such as location and diameter are not correctly reproduced. In

contradiction to that a satisfied reconstruction result can be achieved if the time map takes the base materials shape and its refractive index into account. Two wires with different diameters can be detected in the SAFT image in Figure 7 right. The positions and dimensions of both copper wires are represented in the expected locations on the image.
The SAFT image analysis indicated an increase of the signal to noise ratio by a factor of four in comparison to the measured data. Nevertheless, the pulse trains of the used signals originated from the beam splitter unit (see Figure 6) might cause visible artefacts in the reconstruction image. In the case of air drilled holes (Figure 8 left) the overall signal is lower as in the copper case. The image in Figure 8 indicates the hole positions and sizes as expected although artefacts are more pronounced. There are two reasons for that. First, the signal levels of the pulse train and the reflected pulses become comparable. Second, the back wall reflections of the holes cause for instance a clearly visible inner circle inside the larger drilled hole.

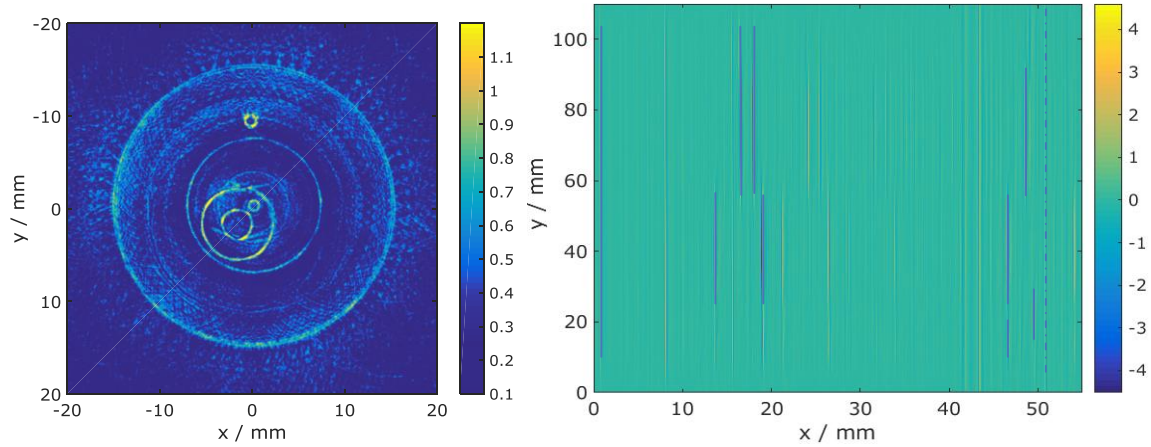

Figure 8: SAFT reconstruction of PE matrix with holes and notches
left: cylindrical sample with drilled holes cylindrical shape was used for time map calculation
right: cuboid scanned with perpendicular incidents angle, the rectangular shape was used for time map calculations

The right side in Figure 8 presents the SAFT image of a cuboid sample scanned parallel to the notches. A time map was used, that took the body material (n=1.5) into account. The positions of the notches relative to the surface were well reproduced. The width of them not, because of the really existing smaller refraction index n=1 inside. For instance the SAFT image indicated notch sizes of 1.3 mm and 5.25 mm instead of the 1.5 mm and 8 mm respectively. An option to overcome these problems can be the optical layer reconstruction approach as described above.

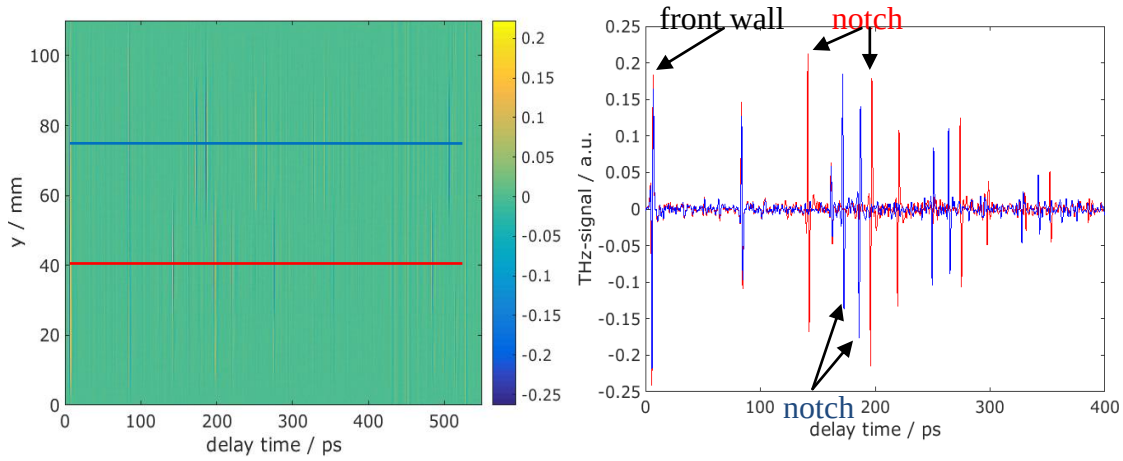

Figure 9: Scan of a cuboid test sample (Figure 5 left)
left: B-scan, perpendicular incidents angle,
right: A-scan along the red e.g. blue line

Figure 9 visualizes the pulse echoes detected during the perpendicular sample scan with the BSU. The test sample (Figure 5 left) represents a three layer system. Any interface initiates one reflection. Additional two delayed echo pulses could be identified originating from the BSU. An optical layer model was used to perform the TD-OLR. The notch thickness could be estimated due to the fit as shown in Figure 10.

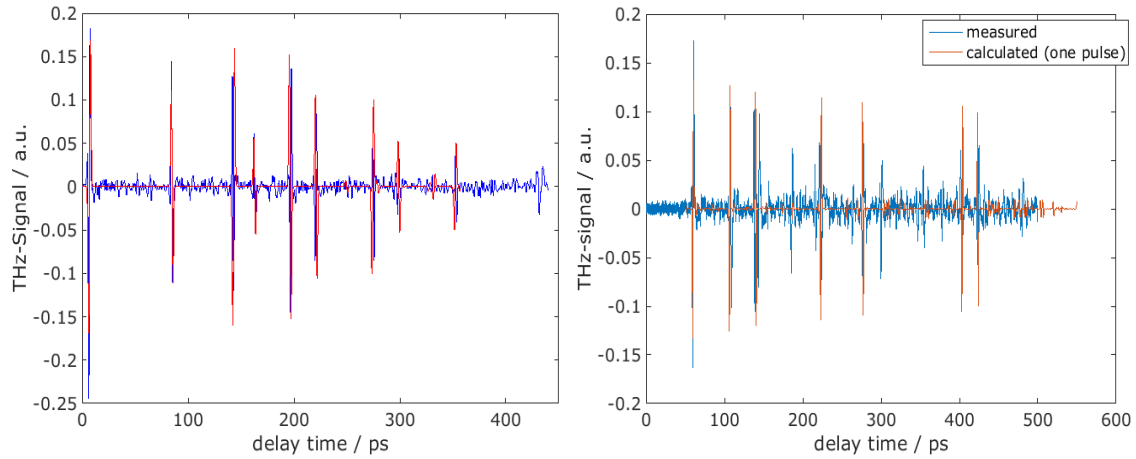

Figure 10: Optical Layer Reconstruction (OLR) fit of A-scan data
left: three pulses train reconstruction of cuboid data from a three layer system (Figure 9 right, red line)
right: single pulse reconstruction of a four layer system (Figure 5 middle)

Summary & Outlook

A THz-time domain SAFT procedure was described and applied on a set of representative test samples. THz - SAFT could increase the SNR by a factor of four in comparison to the raw data. A time map is needed that considers the base materials shape and its refractive index to visualize the inherent features such as copper wires as well as drilled holes properly. It is not possible to reconstruct sizes of layered structures with the presented SAFT algorithm, in case only the samples basic materials (matrix) shape and the refractive index is known. Multiple reflections and unknown refractive index changes in the body material can affect the reconstruction. This is especially observable in notched cuboids. Optical Layer Reconstruction (OLR) was introduced to overcome these problems. A-scan data can be iteratively fitted by this method. A focused beam splitter unit (BSU) was selected to ensure scans directed perpendicular to the samples surface. Unfortunately, BSU results to several echoes with fixed time delays which disturb both THz - SAFT and OLR. The application of a bistatic setup by separating receiver and transmitter could also improve the signal amplitudes and hence the SNR. In case of layered structures SAFT reaches its limits if no additional geometrical and optical parameters for the different layers are available. OLR offers the opportunity to determine the required parameters. In doing so the SAFT algorithm increases in accuracy and reliability in terms of quantitative non destructive testing of dielectric structure components.

References

[1] C. H. Samuel, "3-D Terahertz Synthetic-Aperture Imaging and Spectroscopy," Portland State University, 2013.

[2] S. Wang and X.-C. Zhang, "Pulsed terahertz tomography," *J. Phys. D. Appl. Phys.*, vol. 37, no. 4, pp. R1–R36, Feb. 2004.

[3] M. Spies and W. Jager, "Synthetic aperture focusing for defect reconstruction in anisotropic media," *Ultrasonics*, vol. 41, no. 2, pp. 125–131, 2003.

[4] M. Soumekh, *Synthetic Aperture Radar Signal Processing with MATLAB Algorithms*. New York: Wiley Interscience Publications, 1999.

[5] F. Sanjuan, A. Bockelt, and B. Vidal, "Determination of refractive index and thickness of a multilayer structure with a single terahertz time domain spectroscopy measurement," *Appl. Opt.*, vol. 53, no. 22, pp. 4910–4913, 2014.

[6] J. S. Orfanidis, *Electromagnetic Waves and Antennas*. Rutgers University, 2002.